Available online at www.sciencedirect.com
SCIENCE DIRECT
Bioorganic & Medicinal Chemistry 14 (2006) 1889–1901
Bioorganic & Medicinal Chemistry

# Synthesis and comparative molecular field analysis (CoMFA) of argentatin B derivatives as growth inhibitors of human cancer cell lines

Hortensia Parra-Delgado,[a] César M. Compadre,[b] Teresa Ramírez-Apan,[a] María J. Muñoz-Fambuena,[b] R. Lilia Compadre,[b] Patricia Ostrosky-Wegman[c] and Mariano Martínez-Vázquez[a,*]

[a]*Instituto de Química, Universidad Nacional Autónoma de México, Ciudad Universitaria, Circuito Exterior, Coyoacán, C.P. 04510, México, D.F., Mexico*
[b]*Department of Pharmaceutical Sciences, University of Arkansas for Medical Sciences. Slot 522, 4301 W. Markham, Little Rock, AR 72205, USA*
[c]*Departamento de Medicina Genómica y Toxicología Ambiental, Instituto de Investigaciones Biomédicas, Universidad Nacional Autónoma de México, Ciudad Universitaria, Circuito Exterior, Coyoacán, C.P. 04510, México, D.F., Mexico*

Received 30 August 2005; revised 20 October 2005; accepted 21 October 2005
Available online 10 November 2005

**Abstract**—Synthesis, characterization, anticancer activity, and comparative molecular field analysis (CoMFA) of 14 argentatin B (**1**) analogs are described. The effect of argentatin B derivatives on the growth of K562 (leukemia), PC-3 (prostate), U251 (CNS), and HCT-15 (colon) human cancer cell lines was determined using the sulforhodamine B test. The most active compound in this series, 2-formyl-(16β,24*R*)-16,24-epoxy-25-hydroxycycloart-1-en-3-one (**12**), was about 35–50 times more potent than argentatin B (**1**). Structures were built using the X-ray crystallography of six derivatives for 3D modeling with Sybyl6.9. CoMFA of Log ($1/IC_{50}$) in K562 cell line gave $q^2 = 0.507$, $r^2 = 0.907$, and three components. The standard deviation CoMFA contours indicate that increased activity is associated with a bulky group at C-2, a C1–C2 double bond, and low electronic density at C-25. Experimental Log *P* values for argentatin B and one derivative were 1–2 Log units more hydrophilic than the calculated C Log *P* values.


## 1. Introduction

Triterpenoids form a large class of natural products that, like steroids, are derived from the cyclization of squalene with the retention of all 30 carbon atoms.[1] The group includes members that cover a variety of functional groups and many of these naturally occurring compounds have interesting biological and pharmacological properties.[2] For example, ursolic acid, an ursane-type triterpene, inhibits tumorigenesis[3] and induces tumor cell differentiation.[4] It has also proven effective in the inhibition of angiogenesis[5] and invasion,[6] which are important events involved in tumor metastasis. Additionally, this fact has created an interest in derivatives prepared either by organic synthesis or microbial transformations. For example, several triterpene derivatives that are highly anti-proliferative have been generated.[7]

On the other hand, some cycloartane-type triterpenes[8] such as methyl quadrangulares B and D,[9] and actein[10] have also shown cytostatic and cytotoxic activities on several cancer cell lines.

The cycloartane-type triterpenes named argentatins A and B are the principal components of the resin of the *Parthenium argentatum* Gray. This species, known as Guayule, has been intensively studied as a renewable native source of natural rubber, and it is known that when the rubber is obtained, a by-product named resin is also produced.[11] Taking into account that the argentatins comprise 20 percent of the resins, then these compounds

*Keywords*: Argentatin B; Cytotoxicity; CoMFA; Cycloartanes; Triterpenes; Log *P*.
* Corresponding author. Tel.: +52 55 56224403; fax: +52 55 56162203; e-mail: marvaz@servidor.unam.mx

0968-0896/$ - see front matter © 2005 Elsevier Ltd. All rights reserved.
doi:10.1016/j.bmc.2005.10.038

are available in large amounts. Recently we had demonstrated that argentatin A and some of its derivatives showed antiproliferative activity on several human cancer cell lines.[12] With respect to argentatin B (**1**), we demonstrated that **1** is a non-competitive inhibitor of $^{3}$H-estradiol binding on receptors of hormone-dependent tumors of human breast,[13] and in a previous report, we reported the preliminary evaluation of the effect of **1** on several human cancer cell lines.[14]

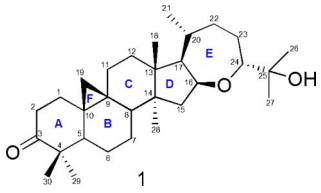


1

Here, to gain insight into the structural requirements in the inhibitory activity of argentatin B (**1**) we synthesized and tested the growth inhibition of 14 analogs in four human cancer cell lines: K562 (leukemia), PC-3 (prostate), U251 (CNS), and HCT-15 (colon).

Hydrophobicity, an established descriptor in the biological activity of numerous chemicals[15] and usually described as the logarithm of a compound's partition coefficient between octanol and water, was calculated with C Log *P*. However, missing parameters for this triterpene produced errors in the calculation and thus we measured experimentally the Log *P*s of two compounds that were available in necessary amounts.

Comparative molecular field analysis (CoMFA) was employed to analyze the quantitative structure-activity relationships of the set of argentatin B analogs. The X-ray geometries of six compounds in the set were templates for conformation and overlapping of molecules (Figs. 1 and 2).

## 2. Chemistry

Syntheses of argentatin B derivatives (**2**–**15**) are shown in Schemes 1 and 2.

The 2-bromo derivative **2** was obtained from argentatin B (**1**) when treated with bromine liquid in acetic acid, while treatment of **1** with phenyl selenium chloride in methylene chloride yielded **3**.

Compound **3** was transformed into the unsaturated acetate **4** by treatment with sodium acetate in acetic anhydride.

Oxime **5** was synthesized by treatment of **1** with hydroxylamine hydrochloride in pyridine. The Beckmann rearrangement of **5** yielded **6**.

Both **1** and **6** were treated with sodium acetate in acetic anhydride to give **8** and **7**, respectively. Acetate **8** was converted to the corresponding oxime **9** by treatment with hydroxylamine hydrochloride in pyridine.

Formyl derivative **10** was achieved from **1** by treatment with sodium methoxide prepared in situ and ethyl formate. In addition, isoxazol derivative **11** was obtained from **10** when treated with hydroxylamine hydrochloride in acetic acid.

Treatment of **10** with phenyl selenium chloride in methylene chloride followed by addition of oxygen peroxide afforded the 1-en-2-formyl argentatin B (**12**).

The reaction of **1** with lithium diisopropylamide and *p*-toluenesulfonic cyanide afforded 2-cyano-argentatin B (**13**).

The unsaturated derivative **14** was obtained from **13** when it was treated with phenyl selenium chloride in methylene chloride followed by the addition of oxygen peroxide.

Lactone **15** was obtained from **1** when it was dissolved in acetic acid and treated with chromium trioxide in water.

All the compounds were characterized by spectroscopic and analytical tools (see Section 4). Additionally, adequate crystals of **1**–**3**, **5**, **10**, and **14**, suitable for X-ray analyses, were obtained. Thus, the structure of such compounds (Fig. 1) was confirmed by X-ray studies. In Table 1 is shown a summary of crystal data and structure refinement for each crystal.

## 3. Results and discussion

The concentration to inhibit 50% cell growth ($IC_{50}$) of argentatin B derivatives (**2**–**15**) (Table 2) in K562 (leukemia), PC-3 (prostate), U251 (CNS), and HCT-15 (colon) human cancer cell lines was determined using the sulforhodamine B test according to a previously established protocol.[16] Preliminary structure–activity relationship observations of the cytotoxicity results showed that a bromine atom substitution at C-2 (**2**) enhanced the potency of argentatin B (**1**) in three cell lines: HCT-15, K562, and PC-3. The C-2 cyano substitution (**13**), improved cytotoxicity of **1** and **2** in all cell lines, however **14**, the unsaturated derivative of **13** was selectively cytotoxic for PC-3 and U251 cell lines showing stronger activity in U251 CNS cancer cells. Compound **12**, a C-1/C-2 unsaturated analog of **13** with an additional formyl substitution at C-2, had a strength 35- to 50-fold higher than **1** and produced the most potent analog in the series. A fused C-2/C-3 isoxazol ring (**11**) decreased cytotoxicity of argentatin B (**1**) in all cell lines. The lactone derivative (**15**) was inactive, suggesting that the presence of an isopropyl alcohol group at C-24 is essential for activity.

CoMFA of Log ($1/IC_{50}$) in K562 cell line of compounds (**1**–**13** and **15**) produced cross-validated $q^2$ value of 0.507 with three components and non-cross-validated $r^2$ of 0.907. The estimated $F$ value was 32.612 and standard

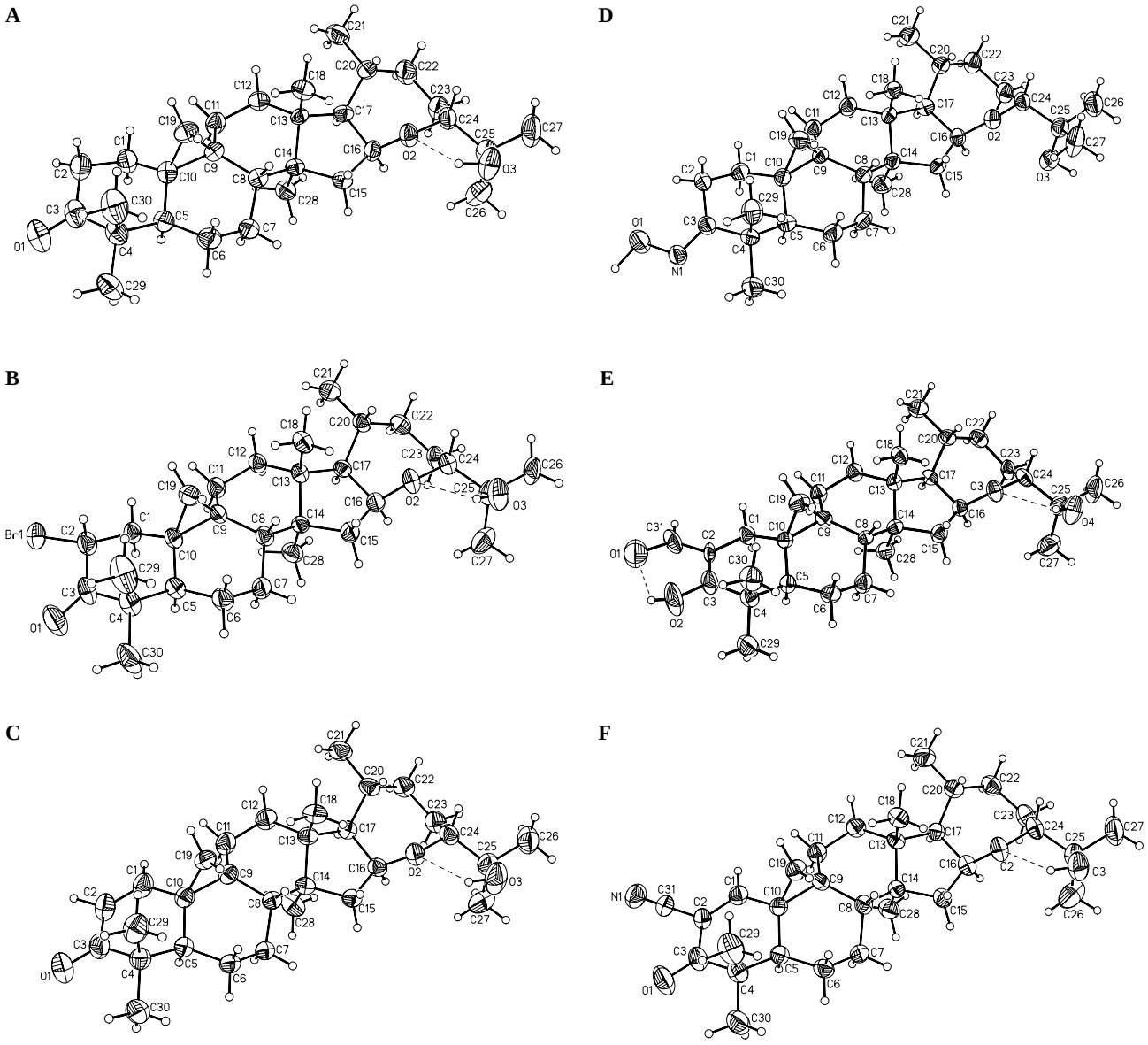


**Figure 1.** Perspective view of molecule crystals. (A) (16β,24*R*)-16,24-Epoxy-25-hydroxycycloartan-3-one (argentatin B, **1**). (B) 2α-Bromo-(16β,24*R*)-16,24-epoxy-25-hydroxycycloartan-3-one (**2**). (C) (16β,24*R*)-16,24-Epoxy-25-hydroxycycloart-1-en-3-one (**3**). (D) 3-Oxime-(16β,24*R*)-16,24-epoxy-25-hydroxycycloartan-3-one (**5**). (E) 2-Formyl-(16β,24*R*)-16,24-epoxy-25-hydroxycycloartan-3-one (**10**). (F) 2α-Cyano-(16β,24*R*)-16,24-epoxy-25-hydroxycycloart-1-en-3-one (**14**). Thermal ellipsoids are drawn at 30% probability levels.

error 0.190. The relative contributions of steric and electrostatic fields were 0.421 and 0.579, respectively. Table 3 lists experimental, predicted, and residual activities of this model (Fig. 3). The standard deviation contours associated with the inhibitory potency of the series produced a relatively large sterically favorable region at C-2 (Fig. 4A, green contour), a small negative yellow contour between C-2 and C-3, and also two smaller negative yellow contours just below the ring. Indeed, molecules **2**, **10**, **12**, and **13** are substituted at C-2 and more active than **1**, however, **11** with a C-2/C-3 fused isoxazol ring is less active than **1**. The smaller yellow contours correspond to the location of hydrogens H-1 and H-2 relates with the fact that **12**, the most potent derivative, has a double bound C1–C2. Still no favorable bulky requirements appeared in the region of the 2-hydroxyisopropyl group attached to C-24, that, with the exception of the inactive **15**, is present in the structures of all derivatives.

CoMFA electrostatic standard deviation map shows a big blue polyhedral surface surrounding atoms C-1 and C-2, indicating that low electronic density at these positions improves the activity (Fig. 4B). This region corresponds to the decreased electronic density at the α,β-unsaturated carbonyls in **3** and **12**; in analogs **2**, **10**, and **13** with electron-withdrawing groups at C-2, all more active than **1**.

Compound **15** lacking a 2-hydroxyisopropyl at C-24 (see Fig. 5B) was inactive in all cell lines; however, CoMFA showed a favorable low electronic density contours around C-25 that was not accompanied by a favorable

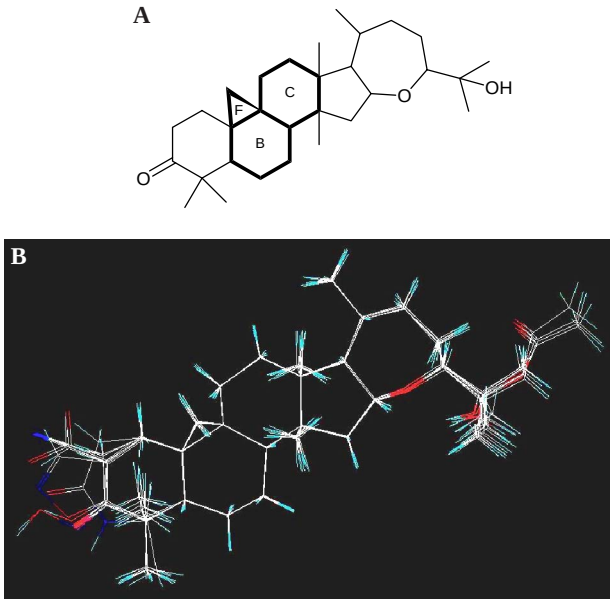


**Figure 2.** (A) Template used for alignment (reference atoms are shown in bold). (B) Training set aligned on **1**.

steric contour. This result suggests that the instability of the lactone ring may be interfering with cytotoxicity rather than a geometrically constrained hydrogen bond donation of 2-hydroxyisopropyl group with a cellular target.

The literature contains numerous reports indicating that lipophilicity is a relevant factor influencing transport, absorption, distribution, and receptor interaction of many chemicals in biological systems. This property parameterized as the logarithm of a compound's partition coefficient between octanol and water, Log *P*, is a descriptor of pharmacodynamic, pharmacokinetic, and toxic aspects of drug activities in QSAR studies.[15] Due to that importance we calculated and also determined the experimental Log *P* values for compounds **1** and **3**. The experimental Log *P* values were $4.3 \pm 0.25$ and $4.8 \pm 0.14$ [see Experimental Section 4.4], while the calculated C Log *P* were 6.42 and 5.74 for **1** and **3**, respectively. The significant differences between predicted and experimental Log *P* values are likely due to the lack of experimental information in the calculating algorithms and emphasize the importance of measuring Log *P*s for natural products for better QSAR studies.

In conclusion, 14 derivatives of argentatin B were obtained by chemical methods. These compounds were spectroscopically characterized and the crystal data for six analogs were also determined. The effect of each compound on growth of several human cancer cells was determined. The biological data for the K562 cell line were used as dependent variable in a comparative molecular field analysis. The results showed that the potency of these triterpenes in K562 increases with bulky substituents at C-2, a C1–C2 double bond, and low electronic density near C-26 and C-27. The experimentally determined Log *P* values of two compounds (**1** and **3**) were 1–2 Log units smaller than those calculated by theoretical methods. These results will be employed to design new bioactive molecules as well as to predict how these triterpenes interact to a yet unknown target which other triterpenes is a nuclear receptor.[17]

## 4. Experimental

### 4.1. Chemistry

Melting points were determined with a Fisher Johns apparatus and are uncorrected. The IR spectra were recorded on a Nicolet FT-55X spectrophotometer. $^1$H NMR spectra were recorded at 200 MHz or 300 MHz (as indicated) on a Varian-Gemini 200, Unity 300, Eclipse 300 Jeol or Bruker-Avance 300 spectrometer. Chemical shifts are expressed in $\delta$ (ppm)

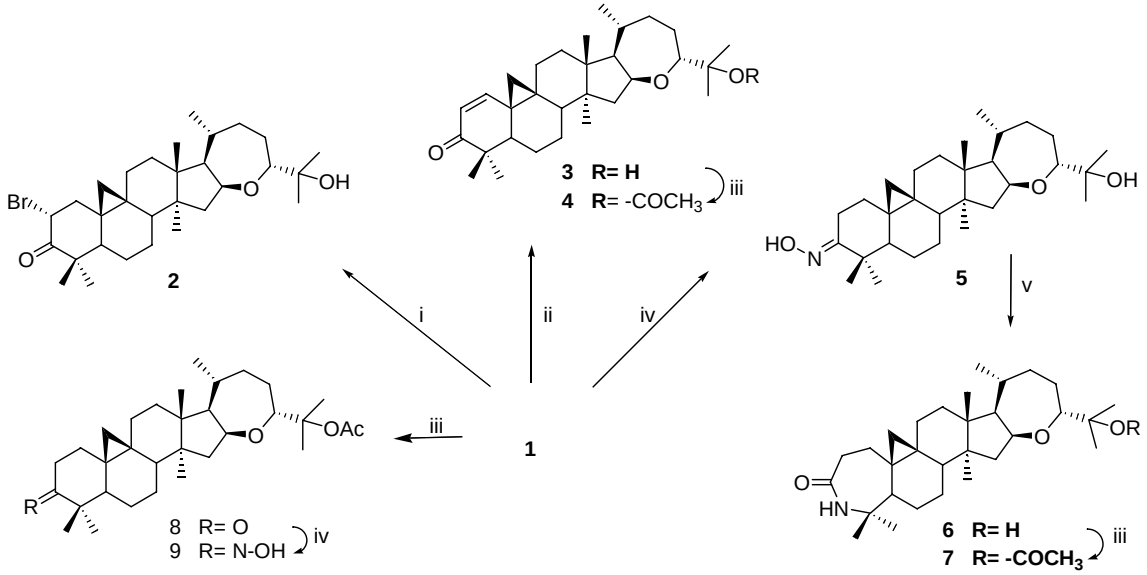


**Scheme 1.** Reagents: (i) Br/$CH_3COOH$, 85.5%; (ii) (a) PhSeCl, EtOAc; (b) THF, $H_2O_2$, 70%; (iii) AcONa/$(CH_3CO)_2O$, 81–89%; (iv) $NH_2OH$·HCl, $C_5H_5N$, 76–78%; (v) TFAA, $CH_2Cl_2$, 53%.

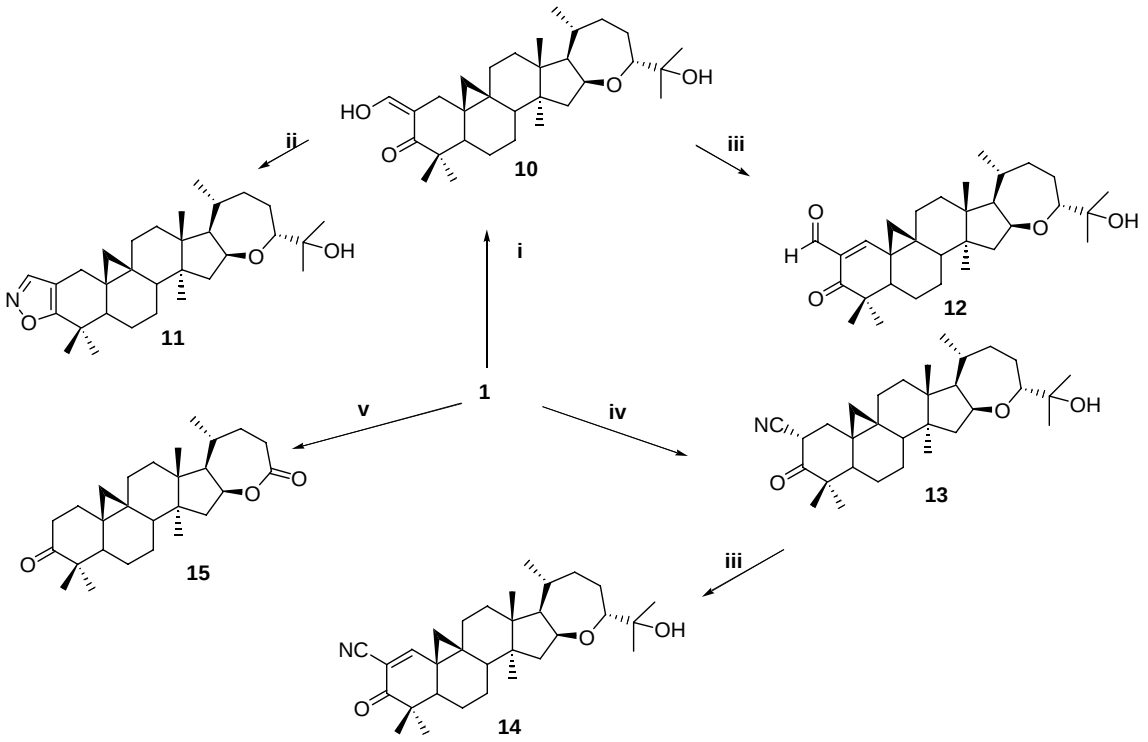


**Scheme 2.** Reagents: (i) $HCO_2Et$, $C_5H_5N$, Na/MeOH, 71%; (ii) $NH_2OH{\cdot}HCl/CH_3COOH$, 80%; (iii) $PhSeCl/CH_2Cl_2/C_5H_5N$, $H_2O_2$, 76–81%; (iv) LDA, *p*-TS-CN, THF, 25–40%; (v) $CH_3COOH$, $CrO_3$, $H_2O$, 45%.

relative to TMS as internal standard and coupling constants *J* in Hz. solvent is indicated for each compound. Mass spectra were recorded on a Jeol AH505HR mass spectrometer. X-ray analysis of some compounds was carried out using a Nicolet P3 ($\lambda = 1.54178$ Å) or a Bruker Smart APEX CCD-based ($\lambda = 0.71073$ Å) diffractometer system (as indicated). Crystallographic data for each structure have been deposited with the Cambridge Crystallographic Data Center (as indicated), Copies of the data can be obtained free of charge on application to The Director, CCDC, 12 Union Road, Cambridge CB2 1EZ, UK (Fax: +44 (1223) 336-033; e-mail for inquiry: deposit@ccdc.cam.ac.uk).

**4.1.1. (16β,24*R*)-16,24-Epoxy-25-hydroxycycloartan-3-one (argentatin B, 1).** The resin, a by-product of the industrial process to obtain natural rubber from *P. argentatum*, was donated by CONAZA Company (Coahuila, Mexico). 157.39 g of the resin was dissolved in a small volume of hexane and percolated over tonsil. The first fractions collected were reunited and their chromatography was carried on silica gel. This procedure resulted in the isolation of argentatin B (8.7 g), which was purified by conventional procedures, and identified by comparison with physical and spectroscopic constants (melting point, $^1H$ and $^{13}C$ nuclear magnetic resonance) with those reported in the literature.[11] Additionally, an X-ray analysis of adequate crystals of argentatin B (**1**) was carried out (Fig. 1A and Table 1). Crystallographic data for the structure have been deposited with the Cambridge Crystallographic Data Center, CCDC 258725.

**4.1.2. 2α-Bromo-(16β,24*R*)-16,24-epoxy-25-hydroxycycloartan-3-one (2).** To a cold solution of 103 mg (0.23 mmol) of **1** in acetic acid was added dropwise with stirring 0.23 mL of 1 M bromine solution in acetic acid. The uptake of bromine was rapid, as evidenced by the fading of the color. After 45 min, the reaction mixture was quenched into ice obtaining a white powder, which was washed with a 5% $NaHCO_3$ solution, filtered, and recrystallized to give 105 mg (85.5%) of product **2**, mp: 156–159 °C. IR ($CHCl_3$) $\nu_{max}$ $cm^{-1}$: 3538.93 (O–H), 2977.18–2874.74 (C–H), 1720.5 (C=O), 1464.44, 1384.73. EIMS *m/z* (%): 534 ($M^+$, 4), 519 ($M^+$-15, 2.7), 476 ($M^+$-58, 26), 475 ($M^+$-59, 47.9), 175 (100), 143 (15.6), 85 (95.2), 59 (76.02). $^1H$ NMR (200 MHz, $CDCl_3$) $\delta$ ppm: 0.71 (d, $J = 4.8$, 1H, H-19), 0.88 (s, 3H, $CH_3$), 0.94 (d, $J = 6.6$, 3H, $CH_3$-21), 1.09 (s, 6H, $2CH_3$), 1.15 (s, 9H, $3CH_3$), 2.80 (br s, 1H, O-*H*), 3.59 (dd, $J = 2.2$, $J = 11.3$, 1H, H-24), 4.60 (q, 1H, H-16). $^{13}C$ NMR (50 MHz) $\delta$ ppm: 33.3 (C-1), 46.0 (C-2), 205.7 (C-3), 55.0 (C-4), 48.4 (C-5), 21.2 (C-6), 20.9 (C-7), 47.4 (C-8), 21.3 (C-9), 26.19 (C-10), 26.4 (C-11), 32.4 (C-12), 45.9 (C-13), 47.5 (C-14), 44.9 (C-15), 74.9 (C-16), 57.4 (C-17), 18.7 (C-18), 29.2 (C-19), 29.2 (C-20), 20.9 (C-21), 35.4 (C-22), 23.4 (C-23), 82.5 (C-24), 73.2 (C-25), 23.9 (C-26), 25.6 (C-27), 19.5 (C-28), 23.0 (C-29), 20.8 (C-30). Furthermore, a colorless prism-like crystal of **2** of approximate dimensions $0.36 \times 0.12 \times 0.09$ mm was used for X-ray analysis. The intensity X-ray intensity data were measured at 291 K on a Bruker Smart System. Crystal data and structure are shown in Table 1 and Figure 1B. Crystallographic data for the structure have been deposited with the Cambridge Crystallographic Data Center, CCDC 258726.

**Table 1.** Summary of crystal data and structure refinement for crystals of molecules **1**, **2**, **3**, **5**, **10**, and **14**

| Compound | **1** | **2** | **3** | **5** | **10** | **14** |
|---|---|---|---|---|---|---|
| Empirical formula | $C_{30}H_{48}O_3$ | $C_{30}H_{47}BrO_3$ | $C_{30}H_{46}O_3$ | $C_{30}H_{49}NO_3$ | $C_{31}H_{48}O_4$ | $C_{31}H_{45}NO_3$ |
| Formula weight | 456.68 | 535.59 | 454.67 | 471.70 | 484.69 | 479.68 |
| Crystal system | Orthorhombic | Orthorhombic | Orthorhombic | Orthorhombic | Orthorhombic | Orthorhombic |
| Space group | $P2_12_12_1$ | $P2_12_12_1$ | $P2_12_12_1$ | $P2_12_12_1$ | $P2_12_12_1$ | $P2_12_12_1$ |
| Unit cell dimensions | | | | | | |
| *A* | 6.3338 (6) Å | 8.2854 (18) | 11.710 (2) | 10.827 (2) | 8.2190 (8) | 8.2357 (6) |
| α (°) | 90 | 90 | 90 | 90 | 90 | 90 |
| *B* (Å ) | 14.049 (1) | 12.129 (3) | 12.128 (2) | 13.366 (3) | 12.4021 (11) | 12.2298 (8) |
| *β* (°) | 90 | 90 | 90 | 90 | 90 | 90 |
| *C* (Å) | 30.046 (3) | 27.310 (6) | 18.811 (4) | 19.105 (4) | 26.535 (3) | 26.854 (2) |
| *γ* (°) | 90 | 90 | 90 | 90 | 90 | 90 |
| Volume (Å$^3$) | 2673.7 (4) | 2744.5 (11) | 2671.5 (9) | 2764.8 (10) | 2704.7 (4) | 2704.8 (3) |
| *Z* | 4 | 4 | 4 | 4 | 4 | 4 |
| Density (calculated) (g/cm$^3$) | 1.135 | 1.296 | 1.130 | 1.133 | 1.190 | 1.178 |
| Absorption coefficient (mm$^{-1}$) | 0.071 | 1.526 | 0.545 | 0.552 | 0.076 | 0.074 |
| *F* (000) | 1008 | 1144 | 1000 | 1040 | 1064 | 1048 |
| *θ* range for data collection (°) | 1.98–25.00 | 1.84–25.00 | 4.34–55.06 | 4.04–55.06 | 1.81–25.00 | 1.83–25.00 |
| Index ranges | $-7 \leqslant h \leqslant 7$<br>$-16 \leqslant k \leqslant 16$<br>$-35 \leqslant l \leqslant 35$ | $-9 \leqslant h \leqslant 9$<br>$-14 \leqslant k \leqslant 14$<br>$-32 \leqslant l \leqslant 32$ | $0 \leqslant h \leqslant 12$<br>$0 \leqslant k \leqslant 12$<br>$0 \leqslant l \leqslant 20$ | $0 \leqslant h \leqslant 11$<br>$0 \leqslant k \leqslant 14$<br>$0 \leqslant l \leqslant 20$ | $-9 \leqslant h \leqslant 9$<br>$-14 \leqslant k \leqslant 14$<br>$-31 \leqslant l \leqslant 31$ | $-9 \leqslant h \leqslant 9$<br>$-14 \leqslant k \leqslant 14$<br>$-31 \leqslant l \leqslant 31$ |
| Completeness to $\theta = 25.00°$ [%] | 99.9 | 100.0 | 99.9 | 97.5[a] | 100 | 100 |
| Data/ restraints/ parameters | 4731/ 0/ 308 | 4841/ 0/ 317 | 1930/ 0/ 308 | 1958/ 0/ 314 | 4772/ 0/ 329 | 4782/ 0/ 326 |
| Goodness-of-fit on $F^2$ | 0.819 | 0.842 | 1.009 | 1.085 | 0.806 | 0.782 |
| Final *R* indices [$I > 2\sigma(I)$] | $R1 = 0.0451$,<br>$wR2 = 0.0472$ | $R1 = 0.0376$,<br>$wR2 = 0.0535$ | $R1 = 0.0405$,<br>$wR2 = 0.1125$ | $R1 = 0.0541$,<br>$wR2 = 0.1388$ | $R1 = 0.0508$,<br>$wR2 = 0.0513$ | $R1 = 0.0456$,<br>$wR2 = 0.0512$ |
| *R* indices (all data) | $R1 = 0.1101$,<br>$wR2 = 0.0547$ | $R1 = 0.0616$,<br>$wR2 = 0.0561$ | $R1 = 0.0431$,<br>$wR2 = 0.1149$ | $R1 = 0.0590$,<br>$wR2 = 0.1429$ | $R1 = 0.1278$,<br>$wR2 = 0.0619$ | $R1 = 0.0992$,<br>$wR2 = 0.0591$ |
| Absolute structure parameter | 1.5 (14) | 0.002 (7) | −0.4 (5) | 0.6 (7) | 0.0 (17) | — |
| Largest diff. Peak and hole [e.Å$^3$] | 0.140 and −0.101 | 0.781 and −0.294 | 0.151 and −0.130 | 0.186 and −0.175 | 0.182 and −0.150 | 0.145 and −0.129 |

[a] $\theta = 55.06°$.

**Table 2.** Effect of argentatin B derivatives on the growth of human cancer cell lines (concentration causing 50% cell growth inhibition)

| Compound | $IC_{50}$ ± SEM (μM) | | | |
|---|---|---|---|---|
| | HCT-15 (colon) | K562 (leukemia) | PC-3 (prostate) | U251 (CNS) |
| **1** | 24.14 ± 5.58 | 79.38 ± 0.08 | 33.41 ± 3.71 | 36.4 ± 6.79 |
| **2** | 12.42 ± 0.91 | 6.03 ± 0.52 | 18.07 ± 2.27 | 39.48 ± 1.75 |
| **3** | 17.04 ± 5.08 | 19.50 ± 4.39 | 35.13 ± 3.90 | 26.19 ± 1.00 |
| **4** | 19.89 ± 5.21 | 50.00 ± 6.10 | 42.19 ± 1.62 | 44.15 ± 2.28 |
| **5** | >100 | 45.81 ± 6.38 | 18.84 ± 3.32 | >100 |
| **6** | >100 | 24.21 ± 2.32 | 59.82 ± 6.51 | 14.75 ± 1.96 |
| **7** | 40.83 ± 4.02 | 29.30 ± 5.26 | 49.82 ± 3.52 | 23.82 ± 6.00 |
| **8** | 27.33 ± 2.35 | 20.38 ± 5.45 | >100 | >100 |
| **9** | >100 | >100 | >100 | 38.89 ± 0.47 |
| **10** | >100 | 23.42 ± 3.43 | 28.13 ± 6.74 | 36.41 ± 3.52 |
| **11** | >100 | >100 | >100 | >100 |
| **12** | 0.44 ± 0.09 | 1.64 ± 0.62 | 0.940 ± 0.001 | 1.05 ± 0.14 |
| **13** | 10.66 ± 2.37 | 4.26 ± 0.65 | 10.28 ± 0.81 | 10.76 ± 0.45 |
| **14** | >100 | >100 | 39.35 ± 5.75 | 19.87 ± 3.72 |
| **15** | >100 | >100 | >100 | >100 |
| Doxorubicin | 0.23 ± 0.01 | 0.28 ± 0.01 | 0.32 ± 0.02 | 0.09 ± 0.02 |

Each data is given as the means ± SEM of at least three independent experiments.

**Table 3.** Observed versus predicted activity (Log $1/IC_{50}$) and residues on CoMFA model for the K562 cell line

| Compound | Log ($1/IC_{50}$) | | CoMFA residuals |
|---|---|---|---|
| | Observed | Predicted | |
| **1** | 4.100 | 4.461 | −0.361 |
| **2** | 5.220 | 5.042 | 0.178 |
| **3** | 4.710 | 4.466 | 0.244 |
| **4** | 4.300 | 4.357 | −0.057 |
| **5** | 4.340 | 4.192 | 0.148 |
| **6** | 4.620 | 4.678 | −0.058 |
| **7** | 4.530 | 4.639 | −0.109 |
| **8** | 4.690 | 4.408 | 0.282 |
| **9** | 4.000 | 4.105 | −0.105 |
| **10** | 4.630 | 4.629 | 0.001 |
| **11** | 4.000 | 4.053 | −0.053 |
| **12** | 5.790 | 5.851 | −0.061 |
| **13** | 5.370 | 5.384 | −0.014 |
| **15** | 4.000 | 4.035 | −0.035 |

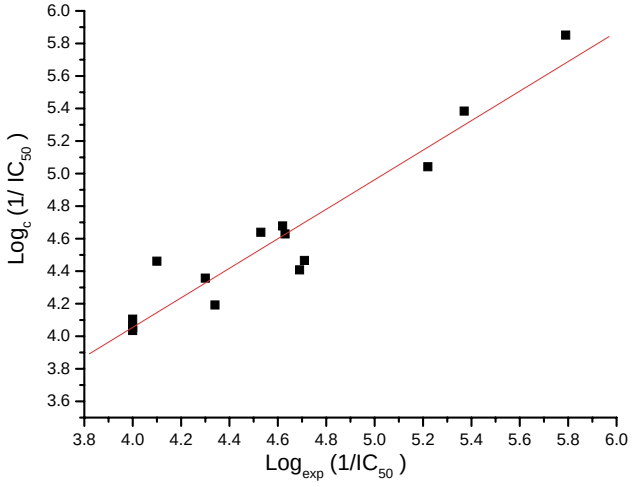


**Figure 3.** Plot of calculated versus experimental Log ($1/IC_{50}$) of CoMFA training set molecules.

**4.1.3. (16β,24*R*)-16,24-Epoxy-25-hydroxycycloart-1-en-3-one (3).** A solution of **1** (200 mg, 0.44 mmol) and phenylselenenyl chloride (100 mg, 0.52 mmol) in EtOAc (4.5 mL) was stirred at room temperature for 2.0 h. To the stirred mixture was added water (1.0 mL). After most of the aqueous layer was removed, THF (2 mL) and 30% $H_2O_2$ (0.2 mL) were added to the organic layer. The mixture was stirred at room temperature for 1.4 h. The mixture was worked up according to the standard method to give a crude solid. The solid was subjected to column chromatography (CC) to give **3** as a crystalline solid (140 mg, 70%). Mp: 165–167 °C. IR ($CHCl_3$) $\nu_{max}$ $cm^{-1}$: 3684.26 (O–H), 3050, 2976.92–2876.12 (C–H), 1663.29 (C=O), 1603, 1521.87, 1473.46, 1424.45, 1334, 1112. EIMS *m/z* (%): 454 ($M^+$, 27), 436 ($M^+$-18, 24), 396 ($M^+$-58, 60), 377 (35), 233 (38), 203 (62), 201 (52), 175 (61), 161 (80), 159 (77), 147 (62), 137 (100), 135 (83), 120 (56), 109 (68), 93 (54), 85 (48) 59 (39).

$^1$H NMR (300 MHz, $CDCl_3$) $\delta$ ppm: 0.75 (d, $J$ = 4.7, 1H, H-19), 0.89 (s, 3H, C$H_3$), 0.94 (d, $J$ = 6.4, 3H, C$H_3$-21),

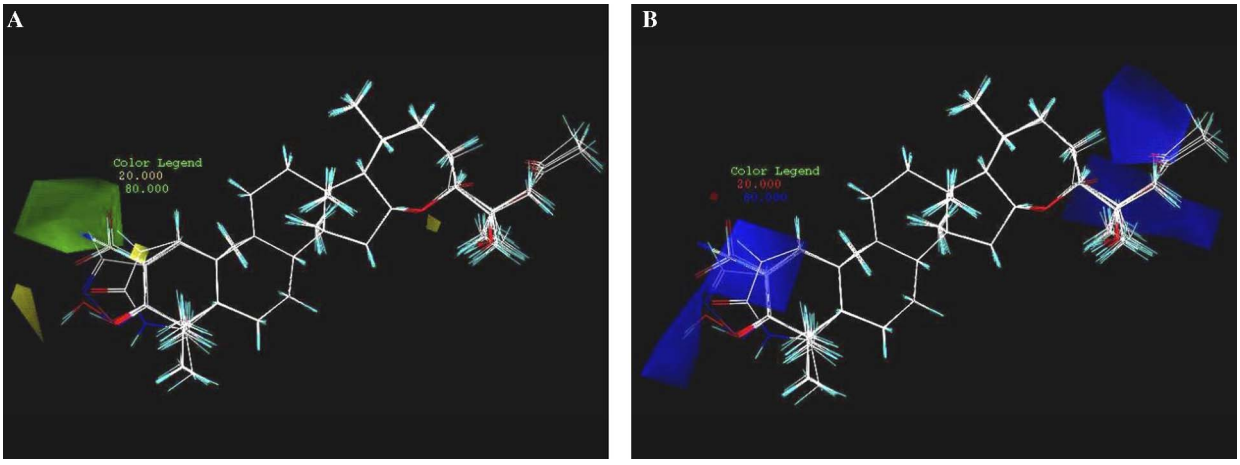


**Figure 4.** (A) CoMFA steric contour plot; green contours indicate regions where bulky groups increase activity, whereas yellow contours indicate regions where bulky groups decrease activity. (B) CoMFA electrostatic contour plots; blue contours indicate regions where positive charge increases activity, whereas red contour indicate regions where negative charge increases activity.

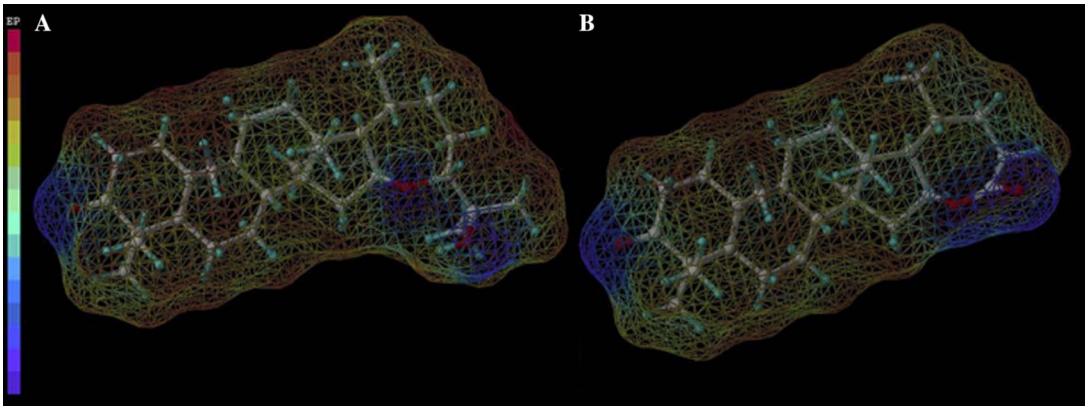


**Figure 5.** Molecular electrostatic potential, color coded, and represented on Connolly surfaces of (A) argentatin B (**1**) and (B) (16*S*,17*R*,20*S*)-3-oxo-25-nor-cycloartan-16,24-lactone (**15**).

0.96 (s, 3H, C$H_3$), 1.09 (s, 6H, 2C$H_3$), 1.10 (s, 3H, C$H_3$), 1.14 (s, 3H, C$H_3$), 1.32 (d, $J$ = 4.7, 1H, H-19′), 2.70 (br s, 1H, O-*H*), 3.60 (dd, $J$ = 2.0, $J$ = 12.5, 1H, H-24), 4.60 (q, 1H, H-16), 5.95 (d, $J$ = 10.0, 1H, H-2), 6.78 (d, $J$ = 10.0, 1H, H-1). $^{13}$C NMR (75.4 MHz) $\delta$ ppm: 153.68 (C-1), 126.77 (C-2), 205.2 (C-3), 46.3 (C-4), 44.4 (C-5), 19.5 (C-6), 27.40 (C-7), 43.2 (C-8), 24.5 (C-9), 29.9 (C-10), 23.6 (C-11), 32.2 (C-12), 45.9 (C-13), 45.8 (C-14), 43.9 (C-15), 74.6 (C-16), 57.0 (C-17), 17.5 (C-18), 29.3 (C-19), 28.4 (C-20), 21.0 (C-21), 35.5 (C-22), 23.4 (C-23), 82.6 (C-24), 73.3 (C-25), 23.9 (C-26), 25.6 (C-27), 18.8 (C-28), 21.4 (C-29), 19.1 (C-30). Furthermore, a pale yellow prism-like crystal of **3** of approximate dimensions 0.50 × 0.50 × 0.20 mm was used for X-ray analysis. The X-ray intensity data were measured at 291 K on a Nicolet P3 diffractometer. Crystal data and structure view are shown in Table 1 and Figure 1C. Crystallographic data for the structure have been deposited with the Cambridge Crystallographic Data Center, CCDC 258727.

**4.1.4. 25-*O*-Acetyl-(16β,24*R*)-16,24-epoxy-25-hydroxy-cycloart-1-en-3-one (4).** A solution of **3** (49 mg, 0.11 mmol) in $Ac_2O$ was treated with sodium acetate (20 mg, 0.24 mmol). The mixture was stirred to reflux for 12 h. The reaction mixture was worked up using conventional procedures to give 44 mg (81%) of **4** as a white solid. Mp: 180–182 °C. IR ($CHCl_3$) $\nu_{max}$ cm$^{-1}$: 2955–2875.65 (C–H), 1726.3 (C=O in acetyl group), 1662 (C=O), 1603.35, 1464.50, 1368.58, 1267, 1115.95. EIMS *m*/*z* (%): 496 ($M^+$, 13), 454 ($M^+$-42, 8), 436 (84), 395 (40), 377 (37), 351 (31), 233 (41), 219 (100), 203 (58), 201 (74), 175 (60), 161 (57), 159 (60), 147 (71), 135 (89), 133 (76), 109 (99), 107 (60), 93 (58), 85 (47), 71 (43), 59 (15), 43 (94).

$^1$H NMR (300 MHz, $CDCl_3$) $\delta$ ppm: 0.74 (d, $J$ = 4.7, 1H, H-19), 0.88 (s, 3H, C$H_3$), 0.93 (d, $J$ = 6.4, 3H, C$H_3$-21), 0.96 (s, 3H, C$H_3$), 1.10 (s, 3H, C$H_3$), 1.13 (s, 3H, C$H_3$), 1.31 (d, $J$ = 4.7, 1H, H-19′), 1.39 (s, 3H, C$H_3$), 1.44 (s, 3H, C$H_3$), 1.96 (s, 3H, C$H_3$), 3.83 (dd, $J$ = 2.2, $J$ = 12.5, 1H, H-24), 4.62 (q, 1H, H-16), 5.94 (d, $J$ = 10.0, 1H, H-2), 6.78 (d, $J$ = 10.0, 1H, H-1). $^{13}$C NMR (75 MHz) $\delta$ ppm: 153.74 (C-1), 127.1 (C-2), 205.2 (C-3), 46.5 (C-4), 44.7 (C-5), 19.8 (C-6), 27.7 (C-7), 43.5 (C-8), 24.8 (C-9), 30.3 (C-10), 23.9 (C-11), 32.5 (C-12), 46.2 (C-13), 46.0

(C-14), 44.1 (C-15), 74.5 (C-16), 57.2 (C-17), 17.8 (C-18), 30.3 (C-19), 22.7 (C-20), 21.7 (C-21), 35.6 (C-22), 22.6 (C-23), 80.5 (C-24), 85.2 (C-25), 21.7 (C-26), 23.5 (C-27), 19.0 (C-28), 21.3 (C-29), 19.4 (C-30), 170.4 and 29.3 (C=O and methyl in acetyl group).

**4.1.5. 3-Oxime-(16β,24*R*)-16,24-epoxy-25-hydroxycycloartan-3-one (5).** Compound **1** (100 mg, 0.22 mmol) in 1.5 mL of pyridine was treated with 28 mg $NH_2OH{\cdot}HCl$ (0.40 mmol) at reflux for 1 h. The mixture was poured into water and extracted with EtOAc. The organic layer was washed with an acid solution followed by water. Oxime **5** was obtained (80 mg, 78%) as a crystal solid, which melted at 224–227 °C. IR (KBr) $\nu_{max}$ $cm^{-1}$: 3496.4, 3387.0 (O–H), 2964.2–2871.9 (C–H), 1645.6, 1460, 1378.6, 1168.8, 1113.4, 928.8. EIMS *m/z* (%): 471 ($M^+$, 78), 454 (65), 413 ($M^+$-58, 40), 412 (90), 396 (50), 107 (38), 59 (100). $^1H$ NMR (300 MHz, $CDCl_3$) $\delta$ ppm: 0.50 (d, $J = 4.5$, 1H, H-19), 0.72 (d, $J = 4.5$, 1H, H-19′), 0.88 (s, 3H, C$H_3$), 0.93 (d, $J = 6.3$, 3H, C$H_3$-21), 1.09 (s, 6H, 2C$H_3$), 1.11 (s, 3H, C$H_3$), 1.15 (s, 3H, C$H_3$), 1.16 (s, 3H, C$H_3$), 3.36 (dq, 1H), 3.59 (dd, $J = 1.8$, $J = 12.5$, 1H, H-24), 4.59 (q, 1H, H-16). $^{13}C$ NMR (75.4 MHz) $\delta$ ppm: 32.7 (C-1), 35.5 (C-2), 168.9 (C-3), 45.8 (C-4), 48.8 (C-5), 21.2 (C-6), 26.1 (C-7), 47.2 (C-8), 20.9 (C-9), 25.6 (C-10), 26.3 (C-11), 32.7 (C-12), 44.8 (C-13), 42.9 (C-14), 45.9 (C-15), 74.9 (C-16), 57.4 (C-17), 18.7 (C-18), 29.5 (C-19), 29.0 (C-20), 20.7 (C-21), 35.5 (C-22), 23.4 (C-23), 82.6 (C-24), 73.3 (C-25), 23.9 (C-26), 25.8 (C-27), 19.5 (C-28), 21.7 (C-29), 20.5 (C-30).

Furthermore, a crystal of **5** of approximate dimensions $0.28 \times 0.24 \times 0.22$ mm was used for X-ray analysis. The X-ray intensity data were measured at 293 K on a Nicolet P3 diffractometer. Crystal data and structure view are shown in Table 1 and Figure 1D. Crystallographic data for the structure have been deposited with the Cambridge Crystallographic Data Center, CCDC 258728.

**4.1.6. 4-Aza-(16β,24*R*)-16,24-epoxy-25-hydroxycycloartan-3-one (6).** Compound **5** (70 mg, 0.15 mmol) in $CH_2Cl_2$ cooled at 0 °C was treated with trifluoroacetic anhydride (1 mL) and the reaction mixture was stirred for 1 h. After water was added, the organic layer was separated and washed with a 5% $NaHCO_3$ solution. The product was purified by CC yielding 38.7 mg of pure lactam **6** that melted at 190–193 °C. IR ($CHCl_3$) $\nu_{max}$ $cm^{-1}$: 3405.1 (O–H), 2963 (C–H), 2871.3, 1650 (CO), 1455.9, 1376.3 (C–N), 1113.0. EIMS *m/z* (%): 471 ($M^+$, 22), 413 ($M^+$-58, 15), 412 (40), 58 (100). $^1H$ NMR (200 MHz, $CDCl_3$) $\delta$ ppm: 0.60 (d, $J = 4.9$, 1H, H-19), 0.67 (d, $J = 4.9$, 1H, H-19′), 0.90 (s, 3H, C$H_3$), 0.93 (d, $J = 6.5$, 3H, C$H_3$-21), 1.09 (s, 6H, 2C$H_3$), 1.15 (s, 3H, C$H_3$), 1.21 (s, 3H, C$H_3$), 1.30 (s, 3H, C$H_3$), 2.56 (m, 2H, C*H*, O*H*), 3.59 (dd, $J = 2.14$, $J = 12.2$, 1H, H-24), 4.61 (q, 1H, H-16), 6.43 (N*H*). $^{13}C$ NMR (50 MHz) $\delta$ ppm: 30.4 (C-1), 35.4 (C-2), 177.6 (C-3), 57.3 (C-4), 50.3 (C-5), 23.5 (C-6), 25.5 (C-7), 48.5 (C-8), 23.0 (C-9), 28.1 (C-10), 26.9 (C-11), 32.9 (C-12), 45.9 (C-13), 45.3 (C-14), 45.1 (C-15), 75.0 (C-16), 57.5 (C-17), 19.1 (C-18), 29.9 (C-19), 28.9 (C-20), 20.9 (C-21), 35.2 (C-22), 25.5 (C-23), 82.6 (C-24), 73.3 (C-25), 23.9 (C-26), 25.7 (C-27), 19.7 (C-28), 31.8 (C-29), 24.3 (C-30).

**4.1.7. 25-*O*-Acetyl-4-aza-(16β,24R)-16,24-epoxy-25-hydroxycycloartan-3-one (7).** A solution of **6** (20 mg, 0.037 mmol) in $Ac_2O$ was treated as for **3** [Section 4.1.4] to give 19.1 mg (89%) of **7** as a white powder which melted at 200–203 °C. IR (KBr) $\nu_{max}$ $cm^{-1}$: 3446.1, 2960 (C–H), 2873.3, 1733.5 (C=O), 1660.3 (C=O), 1458.7, 1371.4, 1255.8, 1115.5. EIMS *m/z*, (%): 513 ($M^+$, 18), 498 (2), 453 (14), 438 ($M^+$-75, 10%), 438 (10), 412 (30), 326 (15), 58 (100), 43 (13). $^1H$ NMR (300 MHz, $CDCl_3$) $\delta$ ppm: 0.60 (d, $J = 4.7$, 1H, H-19), 0.66 (d, $J = 4.7$, 1H, H-19′), 0.90 (s, 3H, C$H_3$-28), 0.92 (d, $J = 6.2$, 3H, C$H_3$-21), 1.14 (s, 3H, C$H_3$-18), 1.23 (s, 3H, C$H_3$-29), 1.31 (s, 3H, C$H_3$-26), 1.39 (s, 3H, C$H_3$-30), 1.44 (s, 3H, C$H_3$-27), 1.96 (s, 3H, C$H_3$ in acetyl moiety), 2.53 (m, 2H, C$H_2$-2), 3.82 (dd, $J = 2.3$, $J = 12.5$ 1H, H-24), 4.63 (q, 1H, H-16), 6.18 (br s, 1H, N*H*). $^{13}C$ NMR (75.5 MHz) $\delta$ ppm: 30.3 (C-1), 34.7 (C-2), 177.9 (C-3), 57.8 (C-4), 50.1 (C-5), 22.2 (C-6), 25.4 (C-7), 48.4 (C-8), 23.1 (C-9), 28.0 (C-10), 26.9 (C-11), 32.8 (C-12), 45.8 (C-13), 45.2 (C-14), 45.1 (C-15), 74.5 (C-16), 57.3 (C-17), 19.1 (C-18), 29.9 (C-19), 28.9 (C-20), 21.0 (C-21), 35.2 (C-22), 25.4 (C-23), 80.1 (C-24), 84.9 (C-25), 24.1 (C-26), 23.2 (C-27), 19.7 (C-28), 31.6 (C-29), 21.3 (C-30), 170.2 and 22.5 (for C=O and methyl in acetyl group).

**4.1.8. 25-*O*-Acetyl-(16β,24*R*)-16,24-epoxy-25-hydroxycycloartan-3-one (8).** Compound **8** was prepared by literature procedures[11] and identified by comparison with physical and spectroscopic constants (melting point, $^1H$ and $^{13}C$ nuclear magnetic resonance) with those previously reported.[11]

**4.1.9. 25-*O*-Acetyl-3-oxime-(16β,24*R*)-16,24-epoxy-25-hydroxycycloartan-3-one (9).** A solution of **8** (100 mg, 0.2 mmol) in pyridine was treated as for **1** [Section 4.1.5] to give 78.3 mg (76%) of **9** as a white powder which melted at 208–210 °C.

IR (KBr) $\nu_{max}$ $cm^{-1}$: 3319.1 (O–H), 2950.3–2874.8 (C–H), 1734.8 (C=O), 1654, 1459.3, 1371.6, 1255.2, 1115.7, 934.5. EIMS *m/z* (%): 513 ($M^+$, 16), 454 (65), 497 (12), 496 (11), 453 (69), 436 (100), 412 (92), 396 (36), 109 (33), 59 (15), 43 (63). $^1H$ NMR (300 MHz, $CDCl_3$) $\delta$ ppm: 0.49 (d, $J = 4.4$, 1H, H-19), 0.72 (d, $J = 4.4$, 1H, H-19′), 0.87 (s, 3H, C$H_3$), 0.92 (d, $J = 6.5$, 3H, C$H_3$-21), 1.12 (s, 3H, C$H_3$), 1.15 (s, 3H, C$H_3$), 1.19 (s, 3H, C$H_3$), 1.39 (s, 3H, C$H_3$), 1.44 (s, 3H, C$H_3$), 1.96 (s, 3H, C$H_3$ in acetyl group), 3.37 (dq, 1H), 3.82 (dd, $J = 2.0$, $J = 12.3$, 1H, H-24), 4.61 (q, 1H, H-16). $^{13}C$ NMR (75.4 MHz) $\delta$ ppm: 32.6 (C-1), 20.8 (C-2), 169.2 (C-3), 43.0 (C-4), 48.7 (C-5), 21.2 (C-6), 25.7 (C-7), 47.1 (C-8), 20.8 (C-9), 26.3 (C-10), 26.1 (C-11), 32.7 (C-12), 45.7 (C-13), 45.6 (C-14), 44.7 (C-15), 74.4 (C-16), 57.2 (C-17), 18.7 (C-18), 29.5 (C-19),

29.0 (C-20), 21.1 (C-21), 35.3 (C-22), 22.3 (C-23), 80.2 (C-24), 85.0 (C-25), 23.5 (C-26), 23.3 (C-27), 19.5 (C-28), 21.7 (C-29), 21.4 (C-30), 170.3 and 22.5 (C=O and methyl in acetyl group).

**4.1.10. 2-Formyl-(16β,24*R*)-16,24-epoxy-25-hydroxycycloartan-3-one (10).** To a solution of 2.88 mmol of **1** in 24 mL of dry pyridine, held under nitrogen, was added 5.0 mL ethyl formate (distilled from phosphorus pentoxide) followed by a solution of 0.44 g of sodium in 6 mL of absolute methyl alcohol. The resulting solution was kept at room temperature under nitrogen overnight. The appearance of a deep color and/ or the formation of an insoluble precipitate evidenced the reaction. The mixture was poured into a cold solution of 16.6 mL of glacial acetic acid in 154.4 mL water, and the resulting precipitate was extracted into methylene dichloride. The organic layer was washed with water and then extracted with a 2% potassium hydroxide solution. The basic extract was washed with ether and acidified with glacial acetic acid. The product (992.9 mg, 71%) was then isolated by extraction in the usual manner. Mp: 210–214 °C. IR (KBr) $\nu_{max}$ $cm^{-1}$: 3546.9 (OH), 3448, 2953.3 (C-H), 2874.5, 1642.9, 1588.2, 1460.3, 1374.2, 1113.1, 1058.2. EIMS *m/z* (%): 484 ($M^+$, 15), 466 (5), 425 ($M^+$-59, 100), 407 (25), 233 (33), 175 (42), 109 (35), 85 (44), 59 (25), 43 (24). $^1$H NMR (300 MHz, $CDCl_3$) $\delta$ ppm: 0.48 (d, $J = 4.5$, 1H, H-19), 0.68 (d, $J = 4.5$, 1H, H-19′), 0.92 (s, 3H, C$H_3$), 0.95 (d, $J = 6.3$, 3H, C$H_3$-21), 1.10 (s, 6H, 2C$H_3$), 1.14 (s, 3H, C$H_3$), 1.18 (s, 3H, C$H_3$), 1.21 (s, 3H, C$H_3$), 1.85 (d, $J = 15$, 1H, H-1), 2.59 (d, $J = 15$, 1H, H-1′), 3.59 (dd, $J = 2.1$, $J = 12.5$, 1H, H-24), 4.61 (q, 1H, H-16), 8.67 (d, $J = 2.4$, 1H, H-31), 14.84 (d, $J = 2.4$, 1H, OH). $^{13}$C NMR (75.4 MHz) $\delta$ ppm: 31.8 (C-1), 106.6 (C-2), 190.4 (C-3), 42.7 (C-4), 48.2 (C-5), 21.4 (C-6), 25.7 (C-7), 44.6 (C-8), 19.4 (C-9), 23.6 (C-10), 25.6 (C-11), 32.6 (C-12), 45.8 (C-13), 45.7 (C-14), 45.1 (C-15), 74.8 (C-16), 57.4 (C-17), 19.1 (C-18), 30.0 (C-19), 29.0 (C-20), 20.9 (C-21), 35.4 (C-22), 23.4 (C-23), 82.5 (C-24), 73.3 (C-25), 23.8 (C-26), 25.6 (C-27), 19.8 (C-28), 24.4 (C-29), 21.6 (C-30), 189.0 (C-31). A colorless prism-like crystal of **10** of approximate dimensions $0.30 \times 0.17 \times 0.07$ mm was used for X-ray analysis. The X-ray intensity data were measured at 291 K on a Bruker Smart diffractometer. Crystal data and structure are shown in Table 1 and Figure 1E. Crystallographic data for the structure have been deposited with the Cambridge Crystallographic Data Center, CCDC 258729.

**4.1.11. [2,3-*d*]Isoxazole-(16β,24*R*)-16,24-epoxy-25-hydroxycycloartane (11).** A solution of 115 mg of **10** in 7 mL glacial acetic acid was stirred and refluxed for 2 h with 45.6 mg of powdered hydroxylamine hydrochloride. The mixture was poured into a cold solution and then extracted with EtOAc. The organic layer was washed with dilute sodium bicarbonate solution to remove acetic acid and then with water. Evaporation of the dried (over anhydrous sodium sulfate) solution and purification by CC afforded 91 mg (80%) of isoxazole **11** that melted at 146–150 °C.

IR (KBr) $\nu_{max}$ $cm^{-1}$: 3482.5 (OH), 3448, 2960.9 (C–H), 2874.5, 1735.1, 1641.3, 1462.8, 1374.7, 1112.9. EIMS *m/z* (%): 481 ($M^+$, 8), 463 (7), 422 ($M^+$-59, 100), 404 (25), 230 (30), 175 (22), 109 (31), 85 (34), 59 (34), 43 (34). $^1$H NMR (200 MHz, $CDCl_3$) $\delta$ ppm: 0.46 (d, $J = 4.8$, 1H, H-19), 0.72 (d, $J = 4.8$, 1H, H-19′), 0.93 (s, 3H, C$H_3$), 0.95 (d, $J = 6$, 3H, C$H_3$-21), 1.10 (s, 6H, 2C$H_3$), 1.18 (s, 3H, C$H_3$), 1.21 (s, 3H, C$H_3$), 1.35 (s, 3H, C$H_3$), 1.95 (d, $J = 15.4$, 1H, H-1), 2.65 (d, $J = 15.4$, 1H, H-1′), 3.60 (dd, $J = 2$, $J = 12.4$, 1H, H-24), 4.62 (q, 1H, H-16), 7.98 (s, 1H, H-31). $^{13}$C NMR (50 MHz) $\delta$ ppm: 28.4 (C-1), 110.0 (C-2), 135.6 (C-3), 45.8 (C-4), 48.3 (C-5), 20.8 (C-6), 26.0 (C-7), 46.7 (C-8), 24.6 (C-9), 29.3 (C-10), 25.6 (C-11), 32.7 (C-12), 45.7 (C-13), 45.7 (C-14), 45.2 (C-15), 74.9 (C-16), 57.5 (C-17), 19.1 (C-18), 30.1 (C-19), 28.9 (C-20), 20.9 (C-21), 35.4 (C-22), 23.5 (C-23), 82.5 (C-24), 73.3 (C-25), 23.9 (C-26), 25.7 (C-27), 19.8 (C-28), 25.5 (C-29), 22.2 (C-30), 149.5 (C-31).

**4.1.12. 2-Formyl-(16β,24*R*)-16,24-epoxy-25-hydroxycycloart-1-en-3-one (12).** To a solution of phenylselenenyl chloride (190 mg) in $CH_2Cl_2$ (7 mL) in an ice bath was added 120 mg pyridine. After 15 min, a cold solution of **10** (100 mg) in $CH_2Cl_2$ (3 mL) was added and the mixture was stirred an additional 20 min. The mixture was washed with 10% aqueous HCl solution twice and cooled back to 0 °C, at which time 0.1 mL of 30% $H_2O_2$ was added. An additional 0.1 mL of 30% $H_2O_2$ was added after 10 min and again after 20 min. After an additional 10 min, 3 mL of water was added. The mixture was worked up according to the standard procedures to give **12** as an amorphous solid (80.2 mg, 81%) that melted at 243–247 °C. IR (KBr) $\nu_{max}$ $cm^{-1}$: 3543.2, 2966.4, 2937.3, 2866.91, 1668.48, 1584.06, 1461.11, 1378.18, 1112.73. EIMS *m/z* (%): 482 ($M^+$, 55), 464 (53), 423 ($M^+$-59, 53), 405 (17), 245 (80), 159 (70), 135 (60), 109 (70), 59 (100), 43 (72). $^1$H NMR (300 MHz, $C_6D_6$) $\delta$ ppm: 0.45 (d, $J = 4.6$, 1H, H-19), 0.60 (s, 3H, C$H_3$), 0.78 (s, 3H, C$H_3$), 0.90 (d, $J = 6.5$, 3H, C$H_3$-21), 0.91 (d, $J = 4.6$, 1H, H-19′), 1.03 (s, 3H, C$H_3$), 1.12 (s, 3H, C$H_3$), 1.14 (s, 3H, C$H_3$), 1.18 (s, 3H, C$H_3$), 2.04 (m, 1H), 2.53 (br s, 1H, O*H*), 3.59 (dd, $J = 3.6$, $J = 12.5$, 1H, H-24), 4.45 (q, 1H, H-16), 7.60 (s, 1H, H-1), 10.51 (s, 1H, H-31). $^{13}$C NMR (75.4 MHz) $\delta$ ppm: 160.6 (C-1), 132.2 (C-2), 201.9 (C-3), 46.2 (C-4), 43.9 (C-5), 19.5 (C-6), 27.7 (C-7), 43.6 (C-8), 27.7 (C-9), 31.5 (C-10), 23.7 (C-11), 32.3 (C-12), 45.8 (C-13), 45.8 (C-14), 44.2 (C-15), 74.5 (C-16), 57.2 (C-17), 17.9 (C-18), 32.1 (C-19), 29.2 (C-20), 21.1 (C-21), 35.7 (C-22), 23.3 (C-23), 82.9 (C-24), 73.0 (C-25), 25.1 (C-26), 25.8 (C-27), 21.5 (C-28), 18.8 (C-29), 18.7 (C-30), 188.9 (C-31).

**4.1.13. 2α-Cyano-(16β,24*R*)-16,24-epoxy-25-hydroxycycloartan-3-one (13).** To 3 mL of a 0.2 M solution of lithium diisopropyl amide (Sigma) at −78 °C under nitrogen was added **1** (250 mg) in dry THF (3.0 mL). The mixture was stirred for 1 h and then the enolate was drawn up by syringe and added to a solution of *p*-toluene-sulfonyl cyanide (368 mg, 2.00 mmol) in THF at −78 °C over a period of about 3 min. The reaction

mixture was stirred for 1 h at −78 °C. After 1 h, the mixture was quenched with concentrated ammonium hydroxide (0.5 mL) and warming the vessel to room temperature to decompose the residual *p*-toluene-sulfonyl cyanide, acidification with 10% HCl, and usual extractive work-up (diethyl ether) afforded the crude product. It was purified by CC and **13** (114 mg) was obtained as an amorphous solid that melted at 222–223 °C. IR (KBr) $\nu_{max}$ $cm^{-1}$: 3544.8 (O–H), 2968.1–2874.0 (C–H), 2251.9 (CN), 1719.7 (C=O), 1463.5, 1370.3, 1114.6, 1058.6. EIMS *m/z* (%): 481 ($M^+$, 3), 422 ($M^+$-59, 74), 404 (100), 336 (15), 175 (52), 161 (32), 133 (30), 109 (43), 85 (50), 59 (35), 43 (24). $^1$H NMR (200 MHz, $CDCl_3$) $\delta$ ppm: 0.67 (d, $J$ = 4.8, 1H, H-19), 0.89 (s, 3H, C$H_3$), 0.94 (d, $J$ = 5, 3H, C$H_3$-21), 1.09 (s, 6H, 2C$H_3$), 1.12 (s, 3H, C$H_3$), 1.13 (s, 3H, C$H_3$), 1.16 (s, 3H, C$H_3$), 2.76 (br s, 1H, O*H*), 3.59 (dd, $J$ = 2.4, $J$ = 12.4, 1H, H-24), 3.93 (dd, $J$ = 5.6, $J$ = 13.1, 1H, H-2β), 4.60 (q, 1H, H-16). $^{13}$C NMR (75.5 MHz) $\delta$ ppm: 38.9 (C-1), 39.9 (C-2), 204.7 (C-3), 50.4 (C-4), 48.5 (C-5), 21.2 (C-6), 25.7 (C-7), 47.1 (C-8), 21.9 (C-9), 25.5 (C-10), 26.4 (C-11), 32.5 (C-12), 45.7 (C-13), 45.7 (C-14), 44.8 (C-15), 74.8 (C-16), 57.4 (C-17), 18.8 (C-18), 29.6 (C-19), 29.0 (C-20), 21.0 (C-21), 35.4 (C-22), 23.5 (C-23), 82.6 (C-24), 73.3 (C-25), 24.0 (C-26), 25.7 (C-27), 19.5 (C-28), 22.2 (C-29), 20.3 (C-30), 117.0 (C-31).

**4.1.14. 2α-Cyano-(16β,24*R*)-16,24-epoxy-25-hydroxycycloart-1-en-3-one (14).** Derivative **14** was obtained using the method previously described in Section 4.1.12. A solution of **13** (40 mg) in $CH_2Cl_2$ was used to give 29.1 mg (76%) of **14** as a crystalline solid which melted at 274–275 °C. IR ($CHCl_3$) $\nu_{max}$ $cm^{-1}$: 3544.27 (O–H), 2957.87, 2876.78, 2232.28 (CN), 1687.55 (C=O), 1594.45, 1464.18, 1385.60, 1113.03. EIMS *m/z* (%): 479 ($M^+$, 21), 461 (36), 420 ($M^+$-59, 45), 402 (60), 375 (25), 336 (30), 233 (68), 219 (47), 201 (24), 175 (44), 161 (90), 147 (74), 135 (64), 109 (100), 94 (73), 85 (78), 81 (51), 59 (51), 43 (57). $^1$H NMR (300 MHz, $CDCl_3$) $\delta$ ppm: 0.88 (s, 3H, C$H_3$), 0.95 (d, $J$ = 6.6, 3H, C$H_3$-21), 1.09 (s, 6H, 2C$H_3$), 1.13 (s, 3H, C$H_3$), 1.13 (s, 3H, C$H_3$), 1.15 (s, 3H, C$H_3$), 3.59 (dd, $J$ = 2.1, $J$ = 12.5, 1H, H-24), 4.61 (q, 1H, H-16), 7.51 (s, 1H, H-1). $^{13}$C NMR (75 MHz) $\delta$ ppm: 166.3 (C-1), 114.0 (C-2), 197.8 (C-3), 46.3 (C-4), 43.8 (C-5), 19.2 (C-6), 27.7 (C-7), 43.3 (C-8), 28.2 (C-9), 32.0 (C-10), 23.2 (C-11), 31.9 (C-12), 45.9 (C-13), 45.8 (C-14), 43.1 (C-15), 74.5 (C-16), 57.0 (C-17), 17.5 (C-18), 31.9 (C-19), 29.0 (C-20), 21.0 (C-21), 35.4 (C-22), 23.4 (C-23), 82.7 (C-24), 73.3 (C-25), 23.9 (C-26), 25.6 (C-27), 21.2, 18.8, 18.6 (C-28 to C-30), 115.4 (C-31). A colorless prism-like crystal of **14** of approximate dimensions 0.32 x 0.16 x 0.07 mm was used for X-ray analysis. The X-ray intensity data were measured at 291 K on a Bruker Smart diffractometer. Crystal data and structure are shown in Table 1 and Fig. 1F. Crystallographic data for the structure have been deposited with the Cambridge Crystallographic Data Center, CCDC 258730.

**4.1.15. (16*S*,17*R*,20*S*)-3-Oxo-25-nor-cycloartan-16,24-lactone (15).** Compound **15** was prepared by literature procedures[11d,e] and identified by comparison with physical and spectroscopic constants (melting point, $^1$H and $^{13}$C nuclear magnetic resonance) with those previously reported.[11d,e]

**4.1.16. (16β,24*R*)-16,24-Epoxy-25-hydroxycycloartan-3,4-lactone (16).** This derivative was prepared in order to obtain a crystalline seven-membered ring-A to be used in the X-ray analysis and it was not evaluated for biological activity. It was synthesized by literature procedures and identified by comparison with physical and spectroscopic constants with those previously reported.[11] An adequate crystal of approximate dimensions 0.6 × 0.5 × 0.06 mm was used for X-ray analysis. Crystallographic data for the structure have been deposited with the Cambridge Crystallographic Data Center, CCDC 258731.

### 4.2. Pharmacology

The inhibitory effects were determined following protocols established by the NCI.[16] The human prostate carcinoma (PC-3), leukemia (K562), central nervous system (U251), and colon carcinoma (HCT-15) cell lines were cultured in RPMI 1640 medium supplemented with 10% fetal bovine serum, 2 mM L-glutamine, 100 IU/ml penicillin, 100 μg/ml streptomycin, and 1% non-essential amino acids. They were maintained at 37 °C in a 5% $CO_2$ atmosphere with 95% humidity. Adherent cells were detached with 0.1% trypsin–EDTA to make single-cell suspensions. Viable cells were counted using a hematocytometer. Cells (5000–10,000 cells/well) were seeded in 96-well microtiter plates and incubated at 37 °C. After 24 h, cells were treated with seven different concentrations (1–100 μM) of the test compounds initially dissolved in dimethylsulfoxide (DMSO, 20 mM) and further diluted in medium to produce the desired concentrations. The plates were incubated for another 48 h at 37 °C. Doxorubicin was used at five different concentrations (0.01–5 μM) as a positive control. After 48 h, adherent cell cultures were fixed in situ by adding 50 μL of cold 50% (wt/vol) trichloroacetic acid and incubated for 30 min at room temperature with 0.4% SRB. Unbound SRB solution was removed washing three times with 1% acetic acid. Plates were air-dried. Protein-bound SRB was dissolved with Tris (tris[hydroxymethyl] aminomethane) buffer and the optical densities were read on an automated spectrophotometric plate reader at a single wavelength of 515 nm. The concentrations required to inhibit cell growth by 50% ($IC_{50}$) were calculated.[16]

### 4.3. Computational details

The inhibitory effect on K562 cancer cell line expressed as Log ($1/IC_{50}$) of the series (Table 2) was used as dependent variable in a comparative molecular field analysis. Compounds were aligned over argentatin B (**1**) as template (Fig. 2). The training set used for the analysis comprised argentatin B and 13 derivatives (**1**–**13**, **15**), compound **14** being detected as outlier during CoMFA.

**4.3.1. Molecular structures.** Compounds **1**–**3**, **5**, **10**, and **14** were built from X-ray crystallographic data. The remaining compounds were obtained with slight modifications of these structures and the standard

bond angles and lengths in Sybyl 6.9 running on silicon graphics Octane®. Energy minimizations were performed using Tripos force field and Mulliken charges.

**4.3.2. Molecular alignment.** The most important requirement for CoMFA studies is that the 3D structures to be analyzed were aligned according to a suitable conformational template, which is assumed to be a 'bioactive conformation.' As no structural information is available about ligand–receptor complexes, compound **1** was used as template structure for the alignment and carbon atoms on cycles B, C, and F were used as common fragment (Fig. 2). Compounds **1**–**13** and **15** were aligned on template by using simple 'align database' option given in Sybyl.

**4.3.3. CoMFA.** Steric and electrostatic interactions were calculated using a $sp^3$ carbon atom as steric probe and a +1 charge as electrostatic probe with Tripos force field. The CoMFA grid spacing was 2.0 Å in the *x*, *y*, and *z* directions. The default value of 30 kcal/mol was set as the maximum steric and electrostatic energy cutoff. Minimum-sigma (column filtering) was set to be 2.0 kcal/mol.

The CoMFA descriptors and Log (1/ $IC_{50}$) were used as independent and dependent variables, respectively, in partial least-square (PLS) regression analyses to derives the 3D-QSAR model. PLS analyses were first conducted using leave-one-out cross-validation method. The final model was developed with the optimum number of components equal to that yielding the highest $q^2$.

### 4.4. Determination of experimental Log *P* of 1 and 3

**4.4.1. Assay.** The experimental Log $P_{ow}$ of **1** was determined at five different concentrations by duplicate (4, 2.5, 2, 1.5, and 1 mg/ ml), using 1 mL octanol (Sigma) and 200 mL of deionized water and GC-MS as detection system. The aqueous phase was extracted with $CH_2Cl_2$ and then it was evaporated, and the residue was transferred to a 100 μL silanized insert in an autosampler vial. The autosampler vial was placed in a manifold to be dried under nitrogen. The dried residue was derivatized with 20 μL MSTFA (*N*-methyl-*N*-trimethylsilyl-trifluoroacetamide) at 75 °C for 20 min.

On the other hand, the experimental Log $P_{ow}$ of **3** was determined at two concentrations by duplicate (2 and 1 mg/ mL), using 1 mL octanol (Sigma) and 200 mL of deionized water. The aqueous phase was extracted with $CH_2Cl_2$ and then it was evaporated under nitrogen. The residue was reconstituted in 30 μL with methanol in an insert, which was placed in an autosampler vial.

**4.4.2. Detection and quantification[18].** An aliquot of 2 μL of sample (**1** or **3**) was used to quantify the compound using GC–MS detection. GC–MS analyses were performed using a HP system (Hewlett-Packard, Palo Alto, CA, USA) consisting of a HP chromatograph connected to a HP 5988 quadrupole mass spectrometer. The GC was equipped with a HP7673 autosampler and a DB-1 column from J&W (Folson, CA, USA). Helium was used as carrier gas with a head pressure of 15 psi. The injector and transfer line were maintained at 285 °C. The column temperature was maintained at 160 °C for 4 min followed by a gradient of 15 °C/min to 230 °C. This temperature was maintained for 4 min and then a gradient of 25 °C/min to 285 °C was carried out. The mass spectrometer conditions were as follows: electron impact, ion source temperature 200 °C, and ionization voltage 62 eV for total ion mode.

Area under the curve (AUC) of the peak at 15.99 (for **1**) or 15.95 min (for **3**) was calculated. Two five-point calibration curves (one for each compound) were used to calculate the milligrams of **1** or **3** in aqueous phase. The milligrams of each compound in octanol phase was then indirectly calculated and concentrations of each compound in each phase led to determine the partition coefficients.

## Acknowledgments

Partial financial support from DGAPA (IN-224802) is acknowledged. We are very grateful to Simón Hernández, Georgina Espinosa, Héctor Ríos, Nieves Zavala, Angeles Peña, Rocío Patiño, Eréndira García, Elizabeth Huerta, Luis Velasco, and Javier Pérez for technical assistance. H.P.D. acknowledges CONACYT and DGEP and DGAPA-UNAM, Mexico, for financial support.

## References and notes

1. Connolly, J. D.; Hill, R. A. *Nat. Prod. Rep.* **1995**, *12*, 609.
2. Tang, W.; Eisenbrand, G. *Chinese Drugs of Plant Origin: Chemistry, Pharmacology, and use in Traditional and Modern Medicine*; Springer: Berlin, 1992.
3. Huang, M. T.; Ho, C. T.; Wang, Z. Y.; Ferraro, T.; Lou, Y. R.; Stauber, K.; Ma, W.; Georgiadis, C.; Laskin, J. D.; Conney, A. H. *Cancer Res.* **1994**, *51*, 701–708.
4. Lee, H. Y.; Chung, H. Y.; Kim, K. H.; Lee, J. J.; Kim, K. W. *J. Cancer Res. Clin. Oncol.* **1986**, *120*, 513–518.
5. Sohn, K. L.; Lee, H. Y.; Chung, H. Y.; Young, H. S.; Kim, K. W. *Cancer Lett.* **1993**, *94*, 213–218.
6. Cha, H. J.; Bae, S. K.; Lee, H. Y.; Lee, O. H.; Sato, H.; Seiki, M.; Park, B. C.; Kim, K. W. *Cancer Res.* **1996**, *56*, 2281–2284.
7. (a) Finlay, H. J.; Honda, T.; Gribble, G. W.; Danielpour, D.; Benoit, N. E.; Suh, N.; Williams, C.; Sporn, M. B. *Bioorg. Med. Chem. Lett.* **1997**, *7*, 1769–1772; (b) Suh, N.; Wang, Y.; Honda, T.; Gribble, G. W.; Dmitrovsky, E.; Hickey, W. F.; Maue, R. A.; Place, A. E.; Porter, D. M.; Spinella, M. J.; Williams, C. R.; Wu, G.; Dannenberg, A. J.; Flanders, K. C.; Letterio, J. J.; Mangelsdorf, D. J.; Nathan, C. F.; Nguyen, L.; Porter, W. W.; Ren, R. F.; Roberts, A. B.; Roche, N. S.; Subbaramaiah, K.; Sporn, M. B. *Cancer Res.* **1999**, *59*, 336–341.

8. (a) Öksüz, S.; Shieh, H.-L.; Pezzuto, J. M.; Özhatay, N.; Cordell, G. A. *Planta Med.* **1993**, *59*, 472; (b) Smith-Kielland, I.; Dornish, J. M.; Malterud, K. E.; Hvistendahl, G.; Romming, C.; Bockman, O. C.; Kolsaker, P.; Stenstrom, Y.; Nordal, A. *Planta Med.* **1996**, *62*, 322–325.
9. Banskota, A. H.; Tezuka, Y.; Kim, P. H.; Qui, T. K.; Saiki, H.; Miwa, Y.; Taga, T.; Kadota, S. *Bioorg. Med. Chem. Lett.* **1998**, *8*, 3519–3524.
10. Saxe, E. L.; Shimizu, M.; Xiao, D.; Nuntanakorn, P.; Lim, J. T. E.; Suzui, M.; Seter, C.; Pertel, T.; Kennelly, E. J.; Kronenberg, F.; Weinstein, I. B. *Breast Cancer Res. Tr.* **2004**, *83*, 221–231.
11. (a) Rodriguez-Hahn, L.; Romo de Vivar, A.; Ortega, A.; Aguilar, M.; Romo, J. *Rev. Latinoamer. Quím.* **1970**, *1*, 24–38; (b) Komoroski, R. A.; Gregg, E. C.; Shockcor, J. P.; Geckle, J. M. *Magn. Reson. Chem.* **1986**, *24*, 534–543; (c) Martínez, R.; Martínez-Vázquez, M.; Zamorano-Macías, O. *Org. Mass Spectrom.* **1990**, *25*, 237–238; (d) Romo deVivar, A.; Martínez- Vázquez, M.; Matsubara, C.; Pérez-Sánchez, G.; Joseph-Nathan, P. *Phytochemistry* **1990**, *29*, 915–918; (e) Martínez-Vázquez, M.; Martínez, R.; Toscano, R. A. *J. Crystallogr.* **1995**, *25*, 331–337.
12. Parra-Delgado, H.; Ramírez-Apan, T.; Martínez-Vázquez, M. *Bioorg. Med. Chem. Lett.* **2005**, *15*, 1005–1008.
13. Calzada, L.; Salazar, E-l; Téllez, J.; Martínez-Vázquez, M.; Martínez, R. *Med. Sci. Res.* **1995**, *23*, 815–816.
14. Parra-Delgado, H.; Ramírez-Apan, T.; Martínez-Vázquez, M. *Rev. Latinoamer. Quím. Suppl.* **2001**, *29*, 76.
15. (a) Poole, S. K.; Poole, C. F. *J. Chromatogr., B* **2003**, *797*, 3–19; (b) Hansch, C.; Leo, A. *Exploring QSAR. Fundamentals and Applications in Chemistry and Biology*; ACS Professional Reference Book: EUA, 1995; (c) Lyman, W. R.; Rosenblatt, D. H. *Handbook of Chemical Property Estimation Methods. Environmental Behavior of Organic Compounds*; Mc Graw-Hill: EUA, 1982.
16. Monks, A.; Scudiero, D.; Skehan, P.; Shoemaker, R.; Paull, K.; Vistica, D.; Hose, C.; Langley, J.; Cronise, P.; VaigroWolff, A.; Gray-Goodrich, M.; Campbell, H.; Mayo, J.; Boyd, M. *J. Natl. Cancer I.* **1991**, *83*, 757–766.
17. Wang, Y.; Porter, W. W.; Suh, N.; Honda, T.; Gribble, G. W.; Leesnitzer, L. M.; Plunket, K. D.; Mangelsdorf, D. J.; Blanchard, S. G.; Willson, T. M.; Sporn, M. B. *Mol. Endocrinol.* **2000**, *14*, 1550–1556.
18. Logsdon, T. W.; Zhou, X.; Breen, P.; Anderson, P.; Gann, L.; Hiller, C.; Compadre, C. M. *J. Chromatogr., B* **1997**, *692*, 472–477.